MICROWAVE ATTENUATION MEASUREMENTS IN 18-23 GHz BAND FOR THE REMOTE SENSING OF THE ATMOSPHERIC WATER VAPOR

F.Cuccoli*, L. Facheris, M. Gherardelli, D. Giuli
Dipartimento Elettronica e Telecomunicazioni, Università di Firenze, Via di Santa Marta, 3 - 50139 Firenze
* email: cuccoli@achille.det.unifi.it, tel +39 055 4796382, fax +39 055 488883

Abstract

The microwave signals propagating in the atmosphere are attenuated due to the presence of gas and water. In particular, around 22.235 GHz (one of the water vapor absorption lines) the power attenuation is dependent on the absorption by atmospheric water vapor that is present up to 20 km altitude from ground. The spectral absorption characteristics of the water vapor are function of temperature, pressure, and water vapor concentration, therefore the spectral properties of the atmosphere change with altitude. Such atmospheric characteristics induced to investigate the use of microwave attenuation measurements in the 18-25 GHz range for remote sensing applications of atmospheric water vapor. In this work some profitable and interesting results are presented about some studies and researches we made about the correlation between spectral attenuation functions and water vapor content along atmospheric propagation paths.

Introduction

Power attenuation measurements in atmosphere are obtainable along a propagation path defined by a transmitter and a receiver. Depending on the location of the transmitter and the receiver, some different remote sensing configurations for the atmospheric water vapor monitoring are possible. Such configurations allow different time space resolution applications. Among these we have:

1. A transmitter located on a Geo-stationary satellite and a receiver located at ground (Fig. 1 (a)). Such configuration makes a fixed vertical propagation link. Therefore the continuous time monitoring of the vertical column of water vapor is possible. A single frequency measurement (19 GHz) is exploitable for the estimation of the total columnar content of water vapor and a multi-frequency measurement can be used to separate the water vapor contribution of the different vertical atmospheric layers.

2. A transmitter located on a LEO/MEO (Low Earth orbit/Medium Earth Orbit)

satellite and a receiver located at ground (Fig. 1 (b)). In this case we can monitor a conical section of the atmosphere made by a single propagation path that scans the vertical conical section (the vertex is the position of the receiver) in a time interval depending on the revisiting time of the satellite. As the previous configuration, a single frequency measurement provides an estimate of the integral content of water vapor along the mobile path and multi-frequency measurements give information about the water vapor contribution of the different vertical atmospheric layers. The relative motion of the satellite with respect to the receiver at ground provides a spatial resolution relatively to the portion of atmosphere that is interested by the propagation during the passing of the satellite.

3. A transmitter located on a LEO/MEO satellite and a set of N receivers placed along a rectilinear line at ground (Fig 1, (c)). This configuration gives a vertical 2D-tomographic network. Instantaneously, we have N parallel propagation paths related to the vertical section of the atmosphere just over the receiver line. During the passage of the satellite, each receiver provides data as in the configuration #2, therefore we have N scans of N vertical conical sections of the atmosphere. Such conical sections are partially overlapped depending on the distance among the receivers at ground. The data related to the overlapped atmospheric sections can be processed by tomographic algorithms to provide the 2D vertical distribution of water vapor. The vertical resolution of the 2D distribution of water vapor is strongly dependent on the number of frequency utilized, while the horizontal resolution depends on the number N of receivers at ground and on their distance. In the LEO case the visibility time is small, therefore the dataset acquired during one passage of the satellite can be considered quasi-stationary with respect to the time variability of the water vapor concentration, therefore the result of the tomographic data processing is a quasi-instantaneous vertical 2D distribution of water vapor.

4. A transmitter located on a LEO/MEO satellite and a receiver located on another LEO/MEO satellite (in general both satellites have the same orbital plane, but different altitude, Fig.1 (e)). In this configuration the propagation path is tangent to the Earth: the tangent altitude (the minimum height from ground of the propagation path) and the path length depend on the relative position between the two satellites. If the satellites rotate in the same direction with the same angular velocity, the path length is constant as well as the tangent altitude; in this case the attenuation measurements are related to the atmospheric layers that are above a constant tangent altitude. The attenuation measurements during the satellite motion are a sampling of the atmosphere that intersects the orbital plane. For a fixed tangent altitude, a single frequency

measurement can provide a suitable estimation of the integral water vapor content, but a multi-frequency approach is preferable. If the satellites rotate in the counter direction the path length and the tangent altitude are variable in time. Moreover, only in selected time intervals the propagation path intersects the atmosphere. During these intervals the tangent altitude rises from 0 to the highest possible value (rise event) or falls from the highest value to 0 (set event). In these conditions the attenuation measurements are related to a scan of the vertical section of the atmosphere. The counter rotating configuration does not allow a single frequency approach for the estimation of the integral water vapor content at all the tangent altitudes. Different tangent altitudes need different frequencies in order to extract the integral water vapor content from the attenuation measurements: therefore, since in the counter rotating configuration the tangent altitude is time dependent, we need more than one frequency.

5. Transmitter and receiver co-located on an airplane or on a satellite (Fig. 1 (d)). In this case we have practically a nadir pointing radar system and we exploit the microwave reflection properties of the Earth's surface. The propagation path is two times the vertical distance between the transmitter/receiver unit and the Earth's surface. As for the configuration #1 we observe the vertical column of the atmospheric water vapor. The relative motion between the transmitter/receiver unit and the Earth's surface allows a mobile vertical propagation path, therefore we scan the vertical section of the atmosphere defined by the nadir track. Also in this configuration single frequency attenuation measurements allow the estimation of the integrated water vapor content.

Configurations 1-3 are oriented to remote sensing applications characterized by the interest in the monitoring of local scale phenomenon, while configuration 4-5 are oriented to global and regional scale applications as meteorology and climatology. However, in all the configuration described above the absorption spectral function we consider is the sensitivity function *S(f)* that is the normalized spectral differential attenuation. Such spectral function allows to emphasize the attenuation contributions that vary with the frequency with respect to all other attenuation effects.

MPM model and sensitivity function

Considering a microwave transmitter-receiver propagation link, the radiative transfer equation providing the power spectral density $P_{tx}(f)$ at the receiver can be written as:

$$P_{rx}(f) = \alpha(f) \cdot P_{tx}(f) \cdot e^{-\tau_a(f)} \tag{1}$$

where f is the frequency, $P_{tx}(f)$ is the transmitted spectral power and $\tau_a(f) = \int_s k_a(s,f)ds$ is the optical depth due to atmospheric absorption, related to the propagation link, $k_a(s,f)$ is the total absorption coefficient, accounting only for energy losses due to molecular absorption, and $\alpha(f)$ accounts for all contributions different from atmospheric absorption. Therefore, it includes also the contribution of the scattering coefficient that, added to the absorption coefficient, gives the extinction coefficient $k(s,f)=k_s(s,f)+ k_a(s,f)$ and the optical depth.

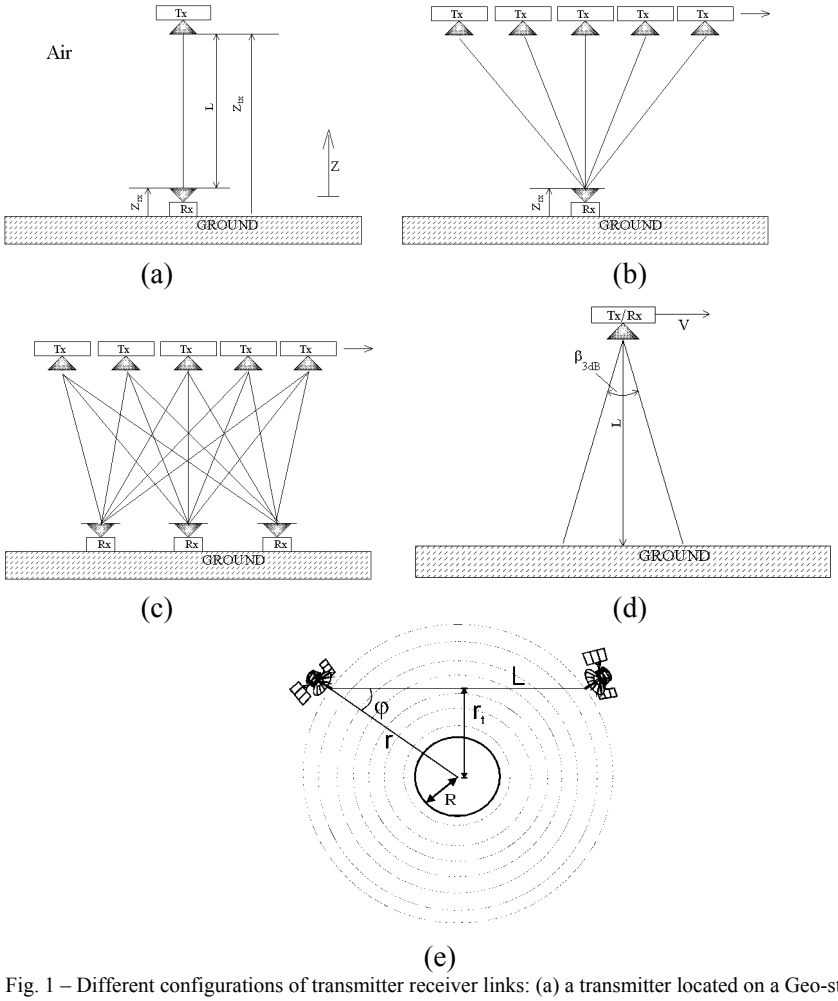

Fig. 1 – Different configurations of transmitter receiver links: (a) a transmitter located on a Geo-stationary satellite and a receiver located at ground, (b) a transmitter located on a LEO/MEO (Low Earth orbit/Medium Earth Orbit) satellite and a receiver located at ground (c) a transmitter located on a LEO/MEO satellite and a set of receivers placed along a rectilinear line at ground (d) mobile vertical microwave link with the transmitter and the receiver located in some place, (e) tangent (limb) microwave link with transmitter and receiver located on two different satellites.

The total absorption coefficient $k_a(s,f)$ can be expressed as summation of all contributions of all the molecular species contained in [s, s+ds]. The MPM93 model by Liebe, utilized throughout this work, includes the following contributions:

- $k_{(O_2)_R}$ O_2 absorption (44 spectral lines up to 834 GHz)
- $k_{(w)_R}$ water vapor absorption (34 spectral lines up to 988 GHz)
- $k_{(O_2)_C}$ O_2 non resonant absorption terms
- $k_{(N_2)_C}$ N_2 non resonant absorption terms
- $k_{(w)_C}$ H_2O continuum spectrum

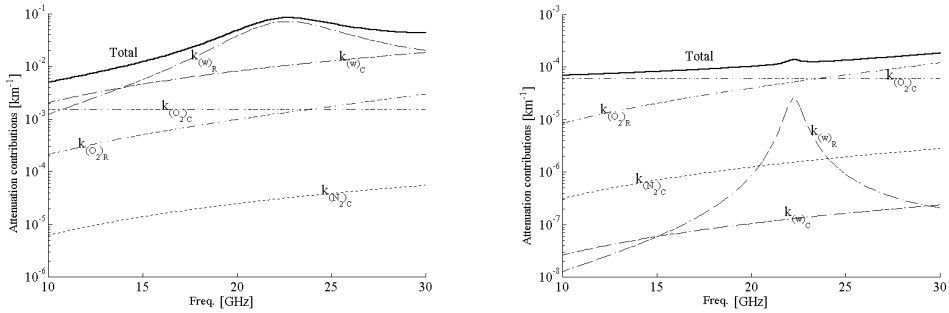

Fig. 2 - Attenuation contributions: (left) at ground (0 km altitude) considering T=294 K, *P*=1013 mb, RH%=80%, (right) at 15 km altitude considering *T*=216 K, *P*=130 mb, RH%=3%.

These contributions depend on temperature *T*, pressure *P* and molecular concentration of water vapor *RH*, O_2 and N_2 . Since pressure of dry air is sufficient to derive N_2 and O_2 contents, barometric pressure, temperature and water vapor concentration are the parameters required to compute/simulate the absorption coefficient through the MPM93.

From eq. (1), the total spectral attenuation for the given MW link is consequently defined as:

$$A(f) = \frac{P_{tx}(f)}{P_{rx}(f)} = \frac{e^{\tau_a(f)}}{\alpha(f)} \tag{2}$$

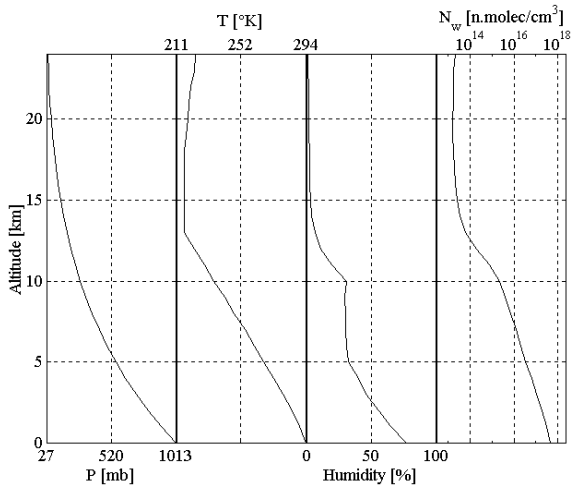

Fig. 3 – Mid Latitude Summer atmospheric model; left to right vertical profiles of: pressure, temperature, relative humidity and water vapor concentration.

Fig. 2 shows the attenuation contributions at ground (0 km altitude) and at 15 km altitude, respectively. Considering the MLS (Mid-Latitude Summer) atmospheric model profiles of Fig. 3, the values of the spectral attenuation have been computed assuming the link geometry of Fig. 1 (a) for the vertical attenuation and the link geometry of Fig. 1 (e) for the horizontal attenuation. Fig. 4 (a) shows the spectral attenuation for the vertical case and Fig 4 (b) and (c) show the spectral attenuation for the horizontal cases in two different tangent altitudes $z_t = r_t - r$ (see parameters in fig 1(e)) and assuming a spherical symmetry hypothesis for the atmospheric composition.

Though the shape of the absorption curves and the attenuation values changes depending on the configuration, it is evident that the shape of the total spectral attenuation is due always to the water vapor absorption effects. Therefore the derivative of the spectral attenuation allows in principle to remove all absorption contributions that are frequency independent and to obtain estimates that are correlated only to the water vapor content.

Let us define the spectral sensitivity function *S(f)* as:

$$S(f) = \frac{1}{A(f)} \frac{d}{df} \left[A(f) \right] \tag{3}$$

Such parameter allows to emphasize the water vapor contribution, exploiting its strong contribution to the first derivative of the spectral attenuation, and to remove all terms that are unknown but that are flat in frequency.

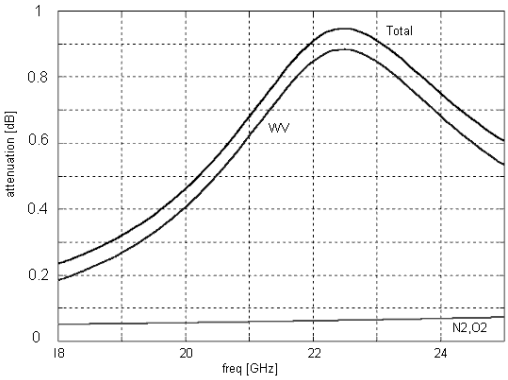

(a)

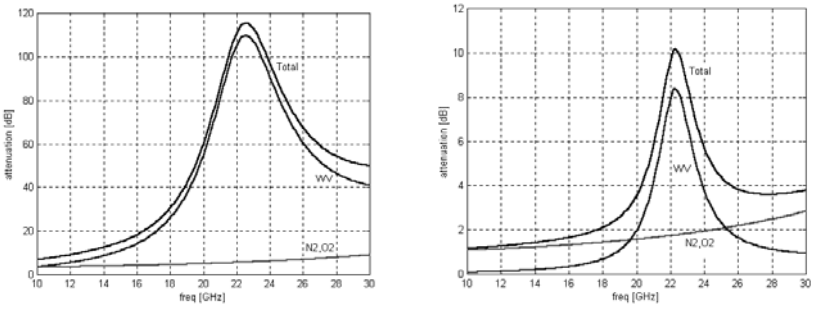

(b) (c)

Fig. 4 – link attenuation considering the MLS atmospheric model shown in Fig. 3: (a) vertical propagation considering the configuration as in fig.1 (a), (b) and (c) horizontal propagation considering the configuration as in fig 1 (e) assuming 0 km altitude (r_t=r) and 6 km altitude (r_t=r+6), respectively

Sensitivity water vapor relationships

In this section we report some results about the relationships between the sensitivity function and the integral content of water vapor considering a set of true radiosonde data. Such data are gathered in S. Piero Capofiume (Bologna, Italy) during one year, therefore they account for all the seasonal variation of atmospheric characteristics in mid latitude areas in terms of vertical profiles of temperature, pressure and water vapor. Radiosonde data provide the quasi-instantaneous vertical profiles of temperature, pressure and water vapor concentration for heights up to 25-30 km. Since in this work we suppose a stratified atmosphere and the spherical symmetry, each atmospheric parameter is only function of the height from ground, therefore a single radiosonde data is sufficient to define the atmospheric parameters along any propagation path, both vertical and horizontal.

For each radiosounding we computed the sensitivity function at 19 and 21 GHz considering both vertical and horizontal propagation paths. Moreover we computed the total water vapor content along the propagation paths.

Fig. 5 summarizes the result of such computation for the vertical case at 19 and 21 GHz. We observe that a quasi deterministic relationship exist between the sensitivity function at 19 GHz and the total content of water vapor, that in this case it is the columnar content (assuming that the path length is at least 15 km), while at 21 GHz a data spread is present. Moreover, at 19 GHz the sensitivity/water vapor relationship is practically linear, therefore the measurement of the sensitivity at 19 GHz allows a direct estimate of the columnar water vapor in vertical propagation paths through a coefficient of proportionality that is computable as linear regression on the data plots like that on the left of Fig 5.

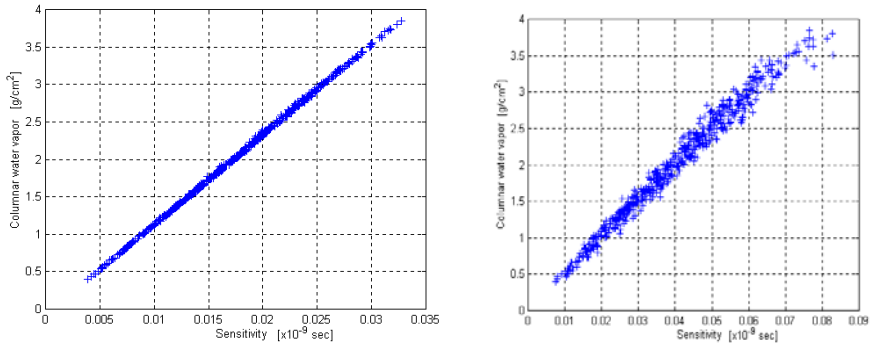

Fig. 5 - Sensitivity *S(f)* versus columnar water vapor content for vertical propagation links (as in fig.1 (a)): (left) sensitivity at 19 GHz; (right) sensitivity at 21 GHz

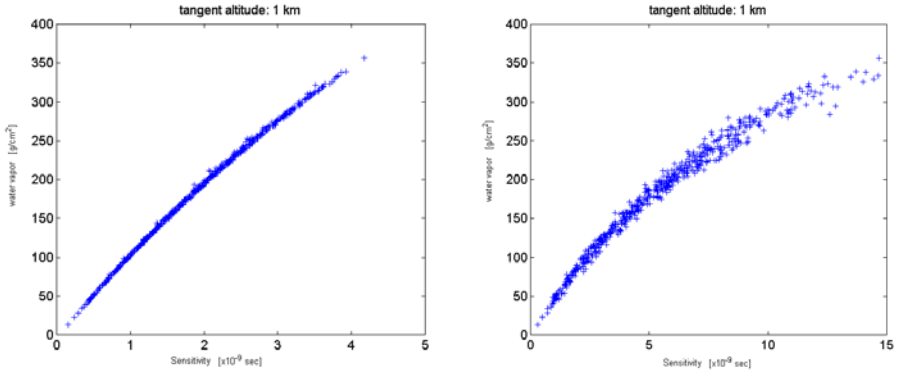

Fig. 6 - Sensitivity *S(f)* versus intregral water vapor content for horizontal propagation links at 1 km altitude (as in fig.1 (e), r_t=r+1 km): (left) sensitivity at 19 GHz; (right) sensitivity at 21 GHz

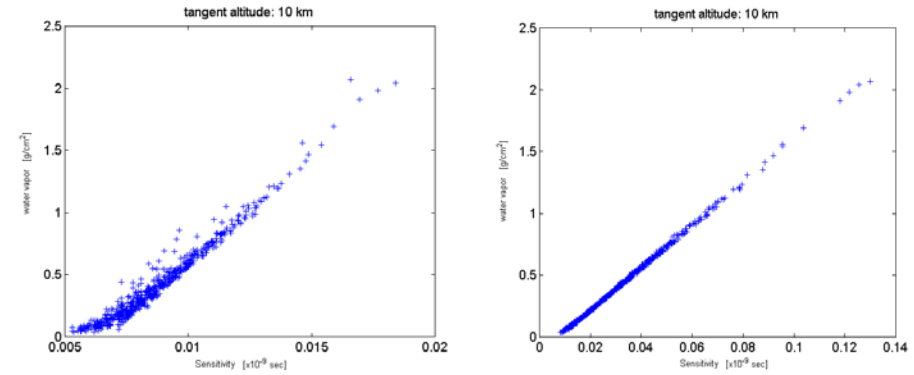

Fig. 7 - Sensitivity S(f) versus intregral water vapor content for horizontal propagation links at 10 km altitude (as in fig.1 (e), r_i=r+10 km): (left) sensitivity at 19 GHz; (right) sensitivity at 21 GHz

Fig 6 and 7 show the results for horizontal propagation links considering two meaningful tangent altitudes: 1 and 10 km. We observe that a quasi deterministic relationship exist between the integral content of water vapor and the sensitivity function at 19 GHz for the case of 1 km tangent altitude (fig 6, on the left) and the integral content of water vapor and the sensitivity function at 21 GHz for the case of 10 km tangent altitude (fig 7, on the right).

While at 21 GHz the sensitivity/water vapor relationship is practically linear for 10 km tangent altitude, at 19 GHz for 1 km tangent altitude the sensitivity/water vapor relationship is not linear. Therefore the estimate of the integral content of water vapor for the lowest tangent altitude using the sensitivity measurements at 19 GHz is still possible, but it requires a non linear regression in order to find out the right law between sensitivity and water vapor. Such non linear regression must be applied on data plots like that on the left of fig 6.

Instead, for 10 km tangent altitude the integral content of water vapor is directly estimable using the measurement of the sensitivity function at 21 GHz through a coefficient of proportionality that is computable as linear regression on the data plots like that on the right of Fig 7. The considerations made for 19 GHz at 1 km tangent altitude are applicable up to 3-4 km and the considerations made for 21 GHz at 10 km are applicable in the 6-11 km range.

Bibliography

1. Cuccoli F.,Facheris L.; "Monostatic CW radar system for microwave attenuation measurements for atmospheric water vapor estimate" ; Geoscience and Remote Sensing Symposium, 2002. IGARSS '02. 2002 IEEE International, Volume: 6 , 2002 Page(s): 3215-3217

2. Cuccoli F., Facheris L.; "Estimate of the tropospherical water vapor through microwave attenuation measurements in atmosphere" ; Geoscience and Remote Sensing, IEEE Transactions on , Volume: 40 Issue: 4, Apr 2002, Page(s): 735 – 741

3. Cuccoli, F.; Facheris, L.; Tanelli, S.; Giuli, D. "Microwave attenuation measurements in satellite-ground links: the potential of spectral analysis for water vapor profiles retrieval"; Geoscience and Remote Sensing, IEEE Transactions on, Volume 39, Issue 3, Page(s): 645-654, March 2001.

4. F.T. Ulaby, R.K.Moore, A.K. Fung, Microwave Remote Sensing, Cap 4, Vol I, Artech House Inc. 1986

5. H.J. Liebe, G.A. Hufford, M.G. Cotton, “Propagation Modeling of Moist Air And Suspended Water/Ice Particles at Frequencies below 1000 GHz”, Presented at an AGARD Meeting on “Atmospheric Propagation Effects through Natural and Man-Made Obscurants for Visible to MM-Wave Radiation”, May 1993

6. Carducci F., Francesi M., "The Italsat Satellite System", International Journal of Satellite Communications, Vol. 13, pp. 49-81, 1995